Porosity Modeling of Huge Thick Carbonates: A Case Study of Lower Paleozoic Carbonates in the Tazhong Uplift, Tarim Basin, China

Chengsheng Chen[1]; Haizu Zhang, Ph.D.[2]; Yunpeng Wang[3]; Lingling Liao, Ph.D.[4]; Shuyong Shi[5]; and Rui Deng[6]

Abstract: This study provides a solution to determine the porosity evolution of huge thick carbonates accurately using PetroMod version 2016.2 software with a cementation tool. The Lower Paleozoic carbonates from the Tazhong Uplift (Tarim Basin) were taken as examples. Results show that the errors of modeled porosity decreased from 256.3%–468.8% to 6.7%–12.5% for low-porosity carbonates and from 15.0%–22.9% to 2.9%–5.0% for high-porosity carbonates, indicating a better fit to the measured values after considering carbonate cementation. The calibrated model incorporating cementation exhibits typically low carbonate porosities and burial depths but high thermal conductivities, resulting in much lower formation temperatures, maturities, and hydrocarbon masses than the uncalibrated model. This study indicated that carbonate cementation plays a very important role in the reduction of carbonate porosity, and it is necessary to calibrate the thick-carbonate porosity model using the cementation tool. Although this method has certain feasibility and practicability and can be utilized widely to model huge thick carbonates, it has a limitation in recovering the increase in porosity caused by postdiagenesis. **DOI: 10.1061/(ASCE)EY.1943-7897.0000798.** © *2021 American Society of Civil Engineers.*

Author keywords: Cementation tool; PetroMod; Huge thick carbonate; Chemical cementation; Ultradeep reservoir.

Introduction

Carbonate diagenesis occurs in four stages: syndeposit, penecontemporaneous shallow burial, medium-deep burial, and postdolomitization. Unlike in the case of other sediments, carbonate porosity reduction is attributed not only to mechanical compaction but also to the chemical cementation that universally occurs in the medium-deep burial stage (Croizé et al. 2013; Schmoker and Halley 1982). In basin modeling, porosity is a critical parameter that directly influences burial depths, rock thermal conductivity, formation pressure and temperature, and retention and migration of geological fluids, thereby finally affecting the model reliability (Hantschel and Kauerauf 2009; Gluyas and Swarbrick 2004; Sekiguchi 1984; Waples and Tirsgaard 2002). Generally, some mechanical compaction algorithms have been embedded and used in basin modeling software for clastic porosity modeling (Walderhaug 2000; Schneider et al. 1996). However, individual mechanical compaction algorithms cannot satisfy the demands of carbonate modeling because chemical cementation can reduce carbonate porosity significantly at specific stages, leading to unacceptable errors in the porosity results (Hantschel and Kauerauf 2009; Gluyas and Swarbrick 2004). For modeling carbonate cementation, the commonly used commercial basin modeling software PetroMod version 2016.2 has an embedded cementation tool. This tool enables users to reconstruct carbonate porosity and its evolution related to chemical cementation. In shallow and thin carbonate rocks, small-scale chemical cementations may not need to be considered because of their weak impact (Hantschel and Kauerauf 2009; Gluyas and Swarbrick 2004). However, in the case of huge, thick, and deep carbonate rocks, which have not been reported or accessed in specific cases, at least in the Tarim Basin, intense chemical cementations must be considered using the cementation tool when modeling because their exclusion results in unacceptable porosity errors.

To meet nergy demands, the focus of the oil and gas exploration strategies in China has shifted to ultradeep (>6,000 m) strata for many years, and many breakthroughs have been achieved, especially in the Tarim Basin. For example, ultradeep light oil, condensate, and natural gas have been identified in the Kuqa (>6,900–7,500 m) and Tabei-Tazhong areas (6,000–8,200 m) of the Tarim Basin, further confirming that this superimposed basin in China has great potential for ultradeep oil and gas exploration (Zhu et al. 2019, 2020, 2021;

[1]Ph.D. Candidate, State Key Laboratory of Organic Geochemistry, Guangzhou Institute of Geochemistry, Chinese Academy of Sciences, Guangzhou 510640, China; Ph.D. Candidate, Univ. of the Chinese Academy of Science, Beijing 100039, China. Email: chenshengcheng14@mails.ucas.ac.cn

[2]Research Institute of Petroleum Exploration and Development, PetroChina Tarim Oilfield Company, Korla 841000, China. Email: zhanghz-tlm@petrochina.com.cn

[3]Professor, State Key Laboratory of Organic Geochemistry, Guangzhou Institute of Geochemistry, Chinese Academy of Sciences, Guangzhou 510640, China (corresponding author). Email: wangyp@gig.ac.cn

[4]Assistant Professor, Guangzhou Institute of Geochemistry, Chinese Academy of Sciences, Guangzhou 510640, China. Email: liaolingling@gig.ac.cn

[5]Ph.D. Candidate, State Key Laboratory of Organic Geochemistry, Guangzhou Institute of Geochemistry, Chinese Academy of Sciences, Guangzhou 510640, China; Ph.D. Candidate, Univ. of the Chinese Academy of Science, Beijing 100039, China. Email: shishuyong15@mails.ucas.ac.cn

[6]Ph.D. Candidate, State Key Laboratory of Organic Geochemistry, Guangzhou Institute of Geochemistry, Chinese Academy of Sciences, Guangzhou 510640, China; Ph.D. Candidate, Univ. of the Chinese Academy of Science, Beijing 100039, China. Email: dengrui16@mails.ucas.ac.cn

Note. This manuscript was submitted on March 8, 2021; approved on July 27, 2021; published online on September 17, 2021. Discussion period open until February 17, 2022; separate discussions must be submitted for individual papers. This paper is part of the ***Journal of Energy Engineering***, © ASCE, ISSN 0733-9402.

Yang 2015, 2020). Present explorations have shown that these ultradeep oil and gas reservoirs are mainly in the Lower Paleozoic Ordovician–Cambrian huge thick carbonates (average thickness greater than 2000 m) widely distributed under the Tarim Basin (Wang et al. 2014; Song et al. 2016; Yang 2015; Zhu et al. 2019). Because of extremely old age and complex geological conditions, either recovering the burial and thermal history or building the petroleum system using basin modeling technology is one of the most important tasks in the comprehensive research of ultradeep reservoirs (Chen et al. 2019; Deng et al. 2019). However, the accurate simulation of the carbonate porosity for such a huge thickness in Tarim Basin has not yet been realized for a specific case, and is the key to building a precise geological model.

This study presents the results of carbonate porosity modeling using PetroMod version 2016.2 with the cementation tool for Well ZS1, which is one of the drillings that produce ultradeep oil and natural gas in the Tazhong carbonate platform (Central Tarim Basin), which has thick-carbonate strata from the Ordovician to Cambrian (>2,800 m) (Wang et al. 2014; Song et al. 2016). Furthermore, we reconstructed the evolution history of carbonate porosity in Well ZS1 after analyzing the carbonate evolutionary stages and burial history using the basin modeling software. We considered the carbonate porosity model of Well ZS1 as a case study to clarify the method of porosity modeling for huge thick carbonates and to explore the difference between cases considering and not considering cementation, thus verifying and emphasizing the significance of precise porosity modeling for thick carbonates.

Geological Setting

Well ZS1 is located in the buried hill zone of the Tazhong Uplift, bounded by the Bachu Uplift to the west, the Gucheng Low Uplift to the east, the Tangguzibasi Depression to the south, and the Manjiar Depression to the north (Fig. 1). The Tazhong Uplift underwent long-term development as an inherited paleouplift caused by fault movement in the Early Caledonian (O_{1-2}) and by fold deformation in the Late Caledonian ($O_3 - S$), forming a basic duplex anticline pattern (Jia 1997; Xiao et al. 2015). The paleouplift reformation period occurred in the Hercynian (D–P), and the local adjustment occurred after the Permian (Su et al. 2011). The evolutionary process was divided into four main stages: paleouplift formation stage, paleouplift construction period, paleouplift reformation period prior to the Carboniferous, and local adjustment in the Late Hercynian (Zhang et al. 2011). Subsequently, the Tazhong Uplift tilted eastward and was denuded along the eastern part; subsequently, it underwent stable settlement to form the present tectonic framework. The sedimentary framework can be classified roughly into four intervals based on depositional and environmental events: the Cambrian to Lower Ordovician strata primarily deposited in carbonate platform environments, the Middle–Upper Ordovician strata deposited in slope environments, the Silurian–Lower Permian strata deposited as marine carbonate and deltaic–fluvial siliciclastic sedimentary rocks during marine transgressions and regressions in foreland-basin environments, and the Upper Permian–Quaternary strata deposited in terrestrial environments

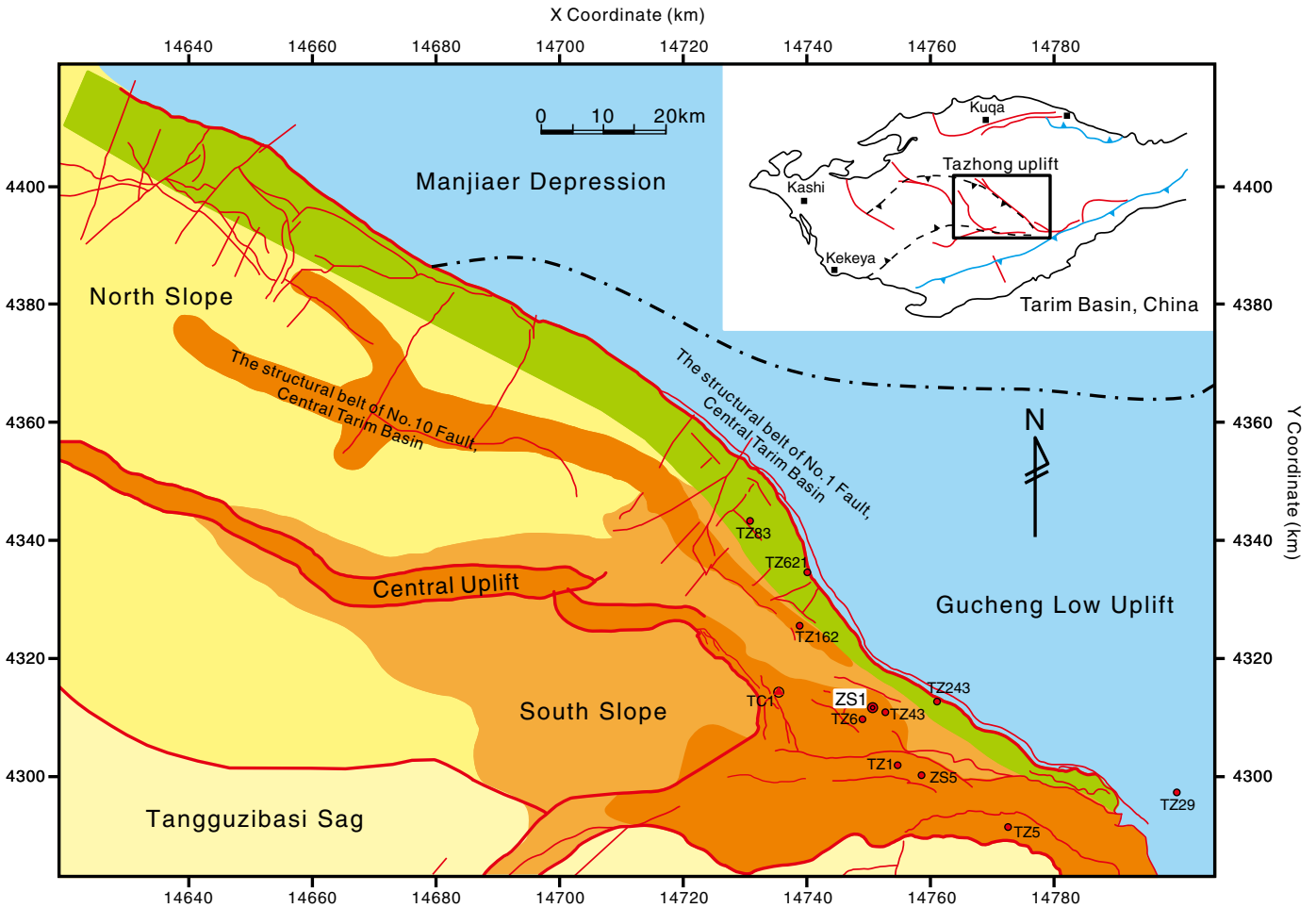

Fig. 1. Structural map of the Tazhong Uplift and the location of Well ZS1. (Adapted from Xiao et al. 2015.)

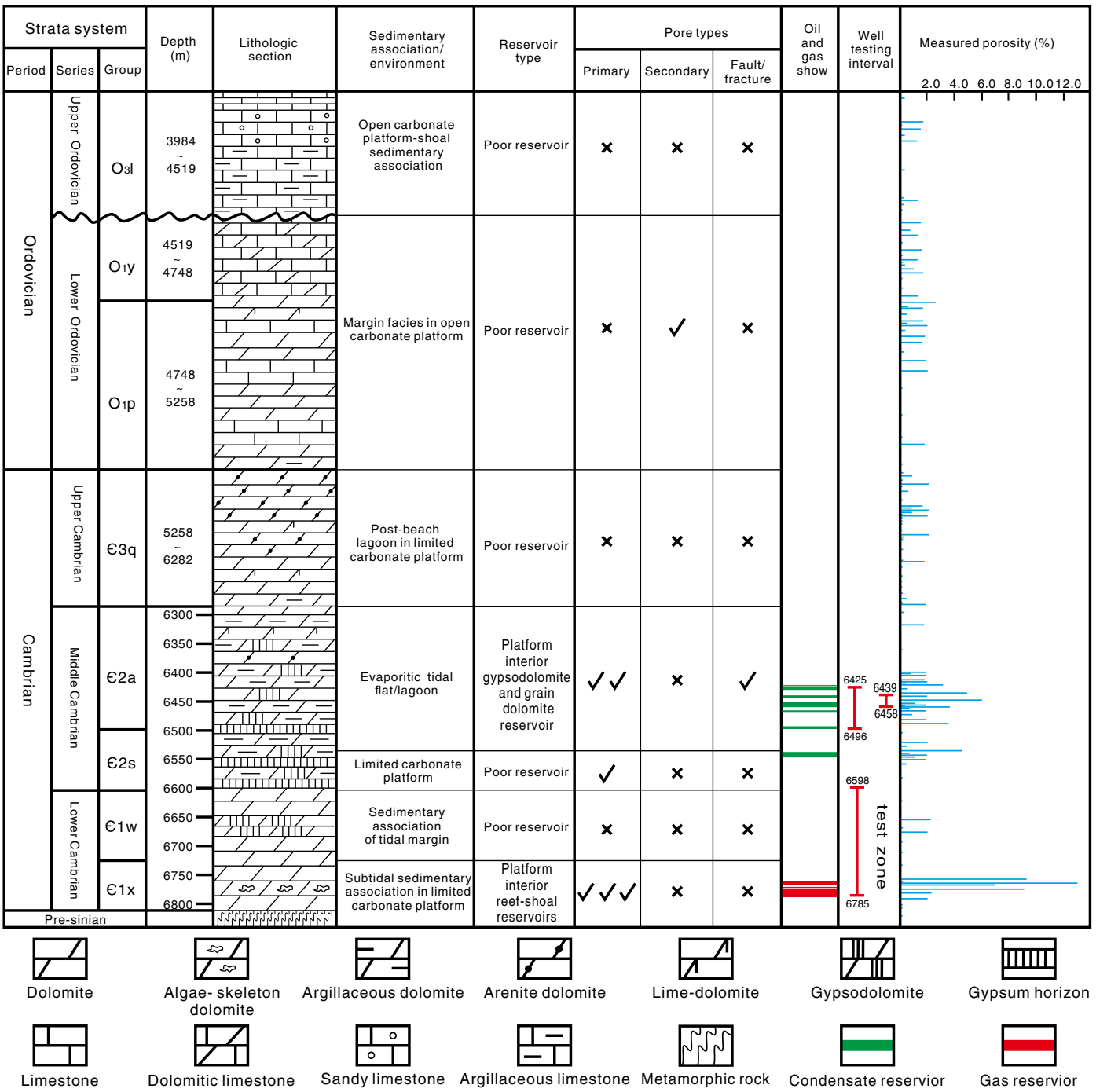

Fig. 2. Simplified stratigraphic column with the porosity characteristics of Well ZS1.

with fluvial–lacustrine facies (Huang et al. 2016; Wang et al. 2014; Zhu et al. 2015).

Gas and condensate were discovered in the Lower Cambrian Xiao'erbulake Formation ($Є_1x$) and Middle Cambrian Awatage Formation ($Є_2a$) in Well ZS1; this discovery was a breakthrough for in-depth petroleum exploration in the subsalt layer of the Cambrian strata. In this well, the cumulative thickness of the Lower Paleozoic carbonate reaches 2,800 m (Wang et al. 2014; Song et al. 2016). Two sets of high-porosity carbonates each are distributed in the Xiao'erbulake Formation ($Є_1x$) and Awatage Formation ($Є_2a$) (Fig. 2). The Xiao'erbulake Formation ($Є_1x$) predominantly comprises algae and grain dolomites, and algal frameworks and intergranular early hypergene dissolution formed the primary pores. The Awatage Formation ($Є_2a$) is composed mainly of gypsodolomite with some fissures and early gypsum-dissolved pores (Shen et al. 2016; Tian et al. 2015). Pores were relatively developed in the Xiao'erbulake Formation ($Є_1x$) and Awatage Formation ($Є_2a$) but were not developed in the other carbonate layers (Fig. 2). The porosity of the whole Lower Paleozoic carbonate ranges from 0% to 12.6%. However, the average porosities of the Xiao'erbulake Formation ($Є_1x$) and the Awatage Formation ($Є_2a$) are 4.5% and 3.6%, respectively, unlike the carbonates in other formations, which are considered low-porosity carbonates (< 2%) (Fig. 2).

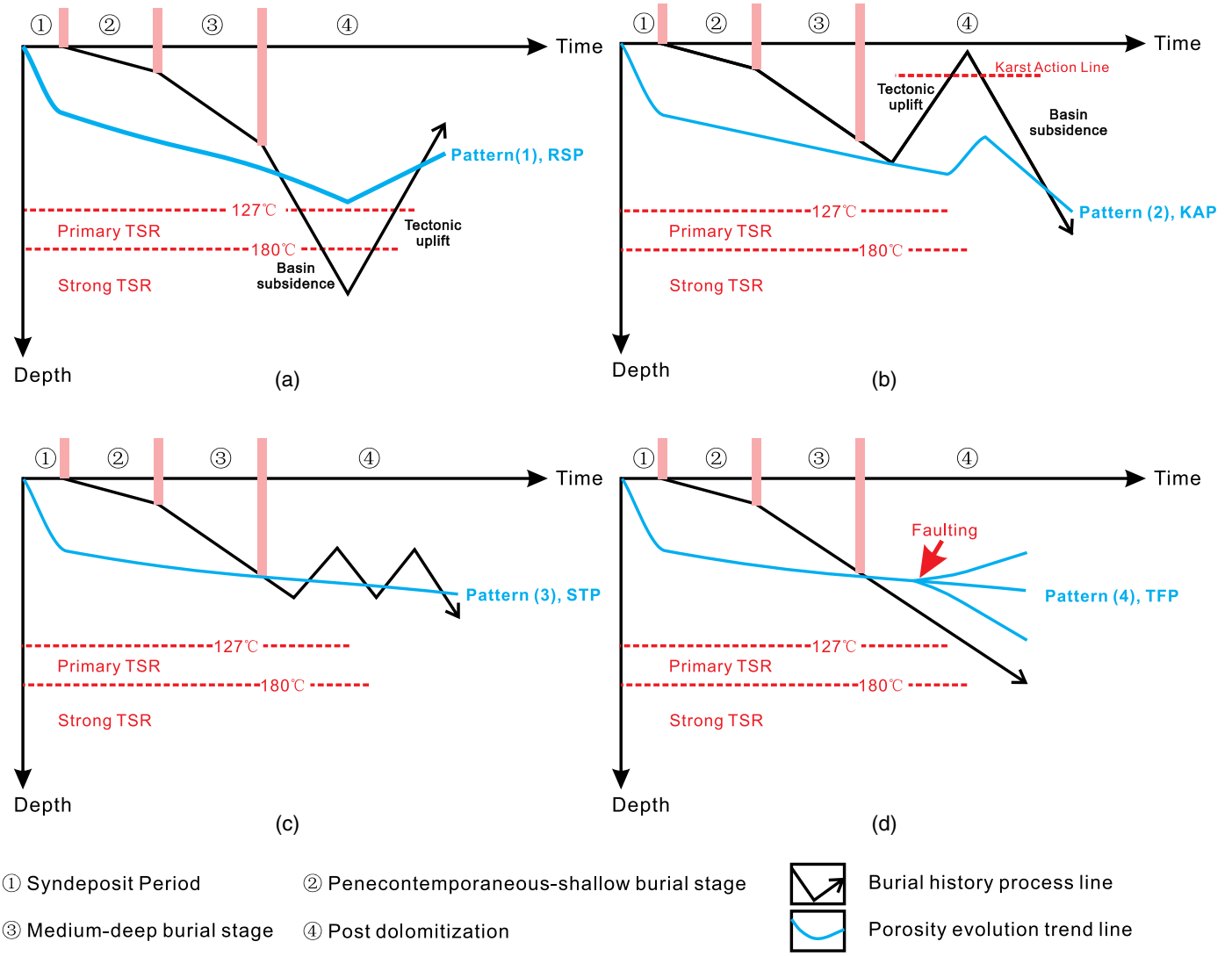

Fig. 3. Carbonate reservoir porosity evolutionary pattern relative to burial history.

Two features of the Middle and Lower Cambrian high-porosity carbonates should be noted: (1) the original pores from the reef–shoal facies and gypsodolomitic sediments contribute considerably to reservoir development; and (2) dolomitization occurred during the penecontemporaneous-shallow period built a solid rock framework, protecting the pores (Shen et al. 2016; Tian et al. 2015). Changes in porosity related to thermochemical sulfate reduction (TSR) should be considered which might contribute to improve reservoir quality (Wang et al. 2014; Zhu et al. 2015; Zhao et al. 2014). For low-porosity carbonates, primary porosity was not developed as cementation occurred widely at historical stages.

Methodology

Carbonate Evolutionary Patterns

Verification of the carbonate evolutionary pattern is critical for modeling carbonate porosity. Four patterns were summarized (Fig. 3): retrograde solubility pattern (RSP), karst action pattern (KAP), stable tectonics pattern (STP), and tectonic faults pattern (TFP) (Jiang et al. 2018; Huang et al. 2010; Zhu et al. 2005; Ma et al. 2008; Wang et al. 2007; Chen 2008).

1. RSP represents deep-to-shallow burial processes. TSR primarily occurs and generates dissolved H_2S and CO_2 in deeper areas and then forms secondary pores in the shallow layer. TSR primarily starts at a temperature of 127°C, and a strong reaction occurs at temperatures over 180°C [Fig. 3(a)] (Machel 2001; Zhu et al. 2005; Wang et al. 2007). The uplift processes boosted the fluid solubility to form secondary pores because the temperatures decreased and affluent H_2S and CO_2 were generated by intense TSR at the greatest buried depth (Huang et al. 2009, 2010; Ma et al. 2008). Finally, the secondary pores were well preserved, improving the reservoir quality because of the enhanced rock mechanics.
2. KAP represents a regional unconformity caused by a large-scale uplift. During the shallow burial period, karstification might have occurred, leading to the formation of secondary pores. When the basin subsided, the porosity decreased [Fig. 3(b)]. If the present buried depth is the greatest, it indicates that continuous subsidences after the paleokarst led to a rise in temperature and carbonate precipitation, causing compaction and severely degrading the reservoir quality because of a heavier overlying load (Huang et al. 2010; Ye et al. 2000; Hantschel and Kauerauf 2009). If this depth was not the greatest, the

Table 1. Key parameters of Well ZS1 used in cementation tool

Layer	Lithology	Initial porosity (%)	Cementation tool table			
			Target porosity (%)	Age (Ma)	Depth (m)	Temperature (°C)
O_3l	Limestone	23	3.0	500	2,000	60.0
O_1y	Dolomitic limestone	23	3.0	500	2,000	60.0
O_1p	Dolomite and limestone	35	3.0	500	2,000	60.0
ϵ_3q	Dolomite	27	3.0	500	2,000	60.0
ϵ_2a	Dolomite and gypsodolomite	26	8.0	500	2,000	60.0
ϵ_2s	Gypsodolomite	24	3.0	500	2,000	60.0
ϵ_1w	Dolomite	35	3.0	500	2,000	60.0
ϵ_1x	Algae-skeleton dolomite	38	15.0	500	2,000	60.0

secondary pores formed by karstification would be maintained and then would form high-quality reservoirs.

3. STP represents a stable tectonic setting in which original pores are dominant owing to a relatively stable tectonic setting. The original pores effectively can be formed and maintained in a penecontemporaneous shallow burial stage before mechanical compaction or pressure solution occurs [Fig. 3(c)]. Statistics show that mechanochemical process can control the rate of sediment compaction at burial depths greater than 1,700 m. In this case, noncemented sediments lose porosity first by mechanical compaction and then reach a locked state at a shallow depth. After mechanical compaction and pressure solution, the dolomite porosity does not decrease clearly without postdolomitization at depths greater than 1,700 m, but maintains a slow decrease with time in the stable condition (Schmoker and Halley 1982; Schmoker et al. 1985; Croizé et al. 2013).
4. TFP refers to the structure-controlled hydrothermal dolomitization by fault systems and includes the processes of compression, extension, and transtension. The hydrothermal fluids preferentially flow upward along extensional and transtensional fault systems, and secondary pores can be formed by the differential dissolution of the original carbonates (mainly limestone). Conversely, a compressional fault system can plug the pores (Chen 2008) [Fig. 3(d)].

In this study, two key characteristics of the Middle–Lower Cambrian high-quality reservoirs in Well ZS1 were observed: the sedimentary original holes in reef–shoal facies and gypsodolomitic sediments that contributed to reservoir development, and the dolomitization that occurred during the penecontemporaneous shallow period and created a solid rock framework to protect the pores (Shen et al. 2016; Tian et al. 2015). In addition, TSR only slightly affected the dolomite owing to the stable tectonics of the lower stratum temperature ($T_{\epsilon 1x} < 180$°C), and hence, the porosity change related to TSR was ignored (Wang et al. 2014; Zhu et al. 2015; Zhao et al. 2014). With respect to the other poor reservoirs, although their primary porosity was not developed, cementation had occurred widely during different historical stages. This analysis showed that STP was the carbonate porosity evolutionary pattern in Well ZS1.

General Procedures

To achieve precise results of carbonate porosity modeling and construct an accurate geologic model, a one-dimensional (1D) basin modeling of Well ZS1 was built using PetroMod 2016.2 software, which allowed us to obtain the approximate thermal and burial histories of this well. The simulation involves the following steps:

1. build a model framework based on the understanding of the geological processes of the basin and region;
2. determine the target layers based on core observation, well reports, and well-logging data; recognize the reservoir types, origin, and distribution of the carbonate; and edit lithologies and initial porosities of the target layer (Table 1);
3. determine the minimum time, depth, and temperature in the case in which cementation occurs and set the target porosity reasonably;
4. fill data in the table of the cementation tool, including the minimum time, depth, and temperature conditions for the assigned layers (only when all required conditions are set can the target porosity modeling be fulfilled);
5. run the simulation and output depth–porosity and time–porosity plots; and
6. calibrate the modeled porosity using the measured data; in the case of bad calibration, return to Step 4 to modify the target porosity values and run the simulation until the porosity modeling results are calibrated reasonably.

Key Parameter Settings

Parameters are the key for porosity modeling using the cementation tool to ensure a good fit between the modeled and measured porosities. Table 1 lists the parameters for the cementation process. The target porosity was derived from the average porosity values. The age represented the start time and was set to 500 million years (Ma). Studies have shown that noncemented sediments first lose porosity via mechanical compaction, reaching a permanent state at a shallow depth. The mechanical compaction and pressure solution of carbonates firmly control the rate of compaction at depths less than 2,000 m. Hence, carbonate porosity, particularly that of dolomite, does not decrease easily after the burial depth exceeds 2,000 m (Croizé et al. 2013; Schmoker and Halley 1982; Schmoker et al. 1985). Because the decrease in carbonate porosity occurs at depths less than 2,000 m, we set this depth as the cementation point in this study to ensure complete cementation. The geothermal gradient of the study area was about 3°C/100 m (Wang et al. 2014).

Results

Cementation and Its Relationship with Burial History

To demonstrate the porosity modeling results, a depth–porosity plot was used. Fig. 4 compares the modeled and measured porosities of the Lower Paleozoic strata for Well ZS1 when the cementation tool was and was not used. The dotted line represents the modeled porosity without the cementation tool, whereas the solid line represents the modeled porosity with the cementation tool. It is evident that the modeling results of the thick carbonate using the cementation tool for Well ZS1 were more consistent with the measured porosity values than were those obtained without using

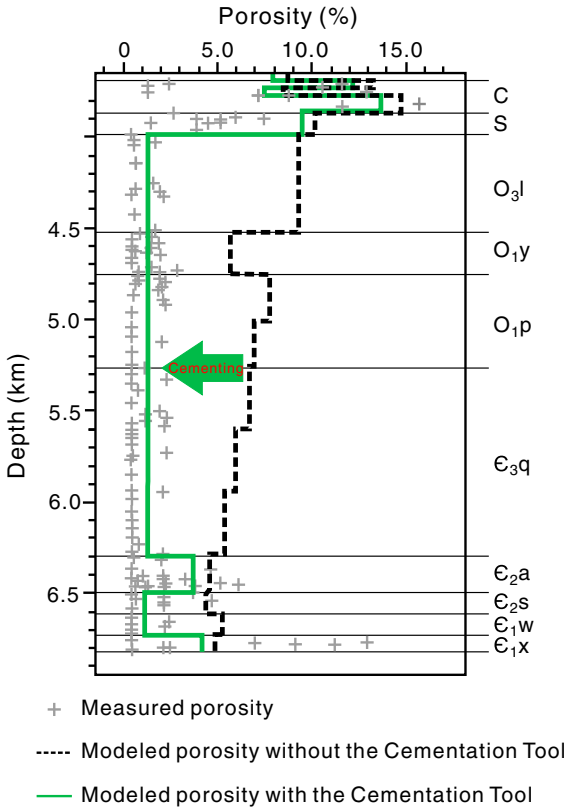

Fig. 4. Modeled and measured porosity results of the Lower Paleozoic strata in Well ZS1 using PetroMod with and without the cementation tool.

the tool (Fig. 4). After calibrating the porosity close to the real porosity, the model was calibrated further to the other parameters that are consistent with the measured parameters, including temperature, maturity, and pressure. All calibration results in Fig. 4 indicate that this model can represent accurately the acutual geological evolution of this area.

The occurrence of cementation typically follows an inherent principle of pressure solution creep, which is controlled by burial depth in geological history (Croizé et al. 2013). Three cementation events occurred in the Early–Middle Ordovician, Silurian, and Permian, corresponding to three subsidence events: the Early Caledonian folding depression (O_{1-2}), the Late Caledonian continuous deep-deposition (S), and the Late Hercynian overall basin subsidence (P), respectively (Fig. 5). This implies that cementation may occur at different ages and to different degrees for different depositional times and depths, although thick-carbonate porosity can decrease rapidly under chemical compaction (cementation). Moreover, the porosity continued to decrease slightly and reached the current values under simple mechanical compaction after cementation (Waples and Tirsgaard 2002; Sun 1995) (Fig. 2; Table 2).

Time–Porosity Plots

The porosity evolution processes can be demonstrated using the time–porosity plot. The results for different strata of Well ZS1 are shown in Fig. 6. These plots clearly illustrate that three cementation events occurred in different stages and layers. The first cementation event occurred in the Early–Middle Ordovician (O_{1-2}), which led to porosity reductions of approximately 8.7%, 77.6%, and 72.6% for $Є_1x$, $Є_1w$, and $Є_2s$, respectively [Figs. 6(a–c); Table 2]. The second cementation event occurred in the Silurian (S), which caused porosity drops of approximately 16.3%, 68.4%,

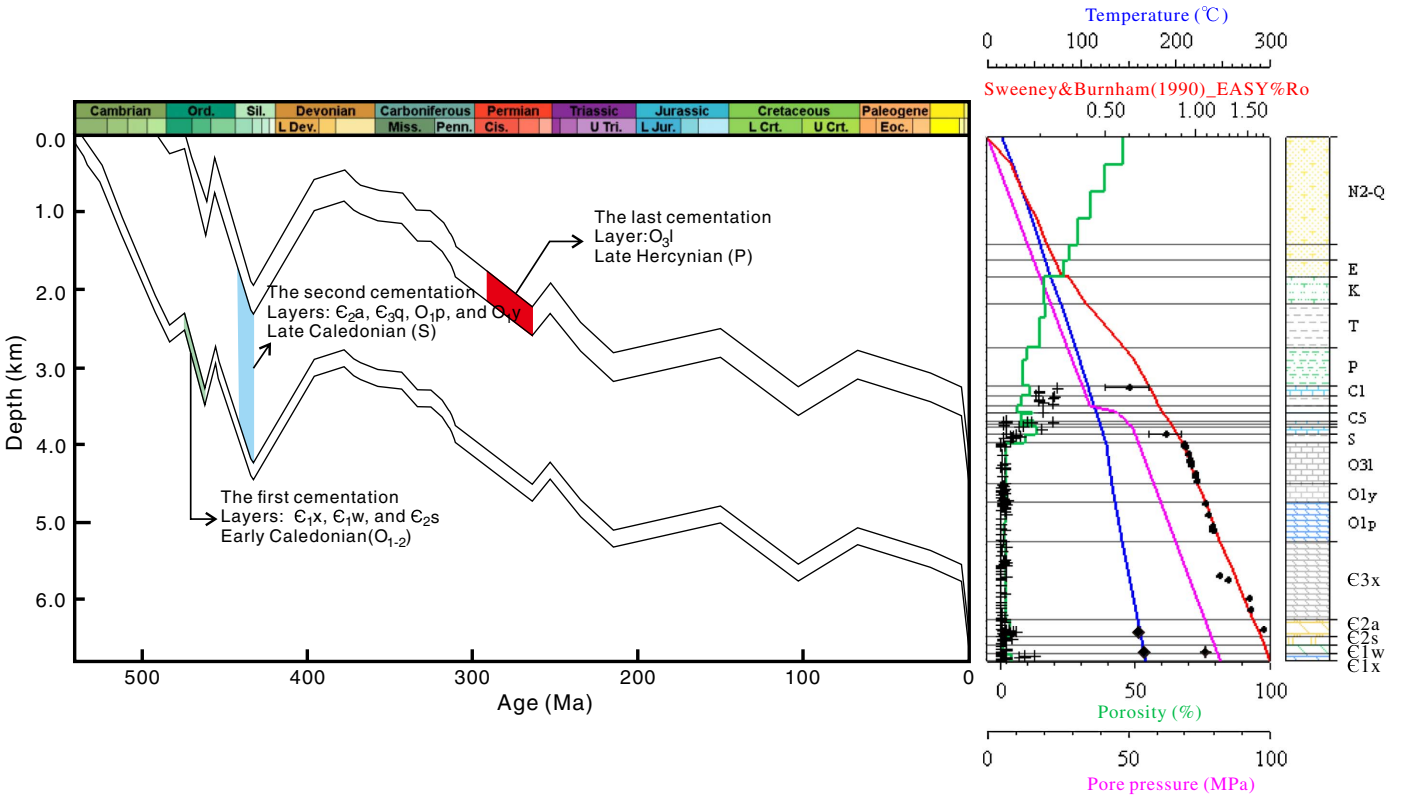

Fig. 5. Relationship between burial history and cementation events along with calibration results.

Table 2. Comparison of modeled porosity (with and without cementation tool) with average measured porosity in each layer

Layer	Modeled porosity without cementation tool, Φ_0 (%)	Modeled porosity with cementation tool, Φ_c (%)	Average measured porosity, Φ_a (%)	Reduction, p (%)	Error rate without cementation tool, σ_0 (%)	Error rate with cementation tool, σ_c (%)	Porosity level
O_3l	9.1	1.8	1.6	80.2	468.8	12.5	Low-porosity
O_1y	5.4	1.6	1.5	70.3	260.0	6.7	
O_1p	6.7	1.6	1.5	76.1	346.7	6.7	
ϵ_3q	5.7	1.8	1.6	68.4	256.3	12.5	
ϵ_2a	4.3	3.6	3.5	16.3	22.9	2.9	High-porosity
ϵ_2s	4.0	1.1	1.0	72.5	300.0	10.0	Low-porosity
ϵ_1w	4.9	1.1	1.0	77.6	390.0	10.0	
ϵ_1x	4.6	4.2	4.0	8.7	15.0	5.0	High-porosity

Note: $p = (\Phi_0 - \Phi_c)/\Phi_0 \times 100\%$; $\sigma_0 = (\Phi_0 - \Phi_a)/\Phi_a \times 100\%$; $\sigma_c = (\Phi_c - \Phi_a)/\Phi_a \times 100\%$.

76.1%, and 70.4% for ϵ_2a, ϵ_3q, O_1p, and O_1y, respectively [Figs. 6(d–g); Table 2]. The final cementation event occurred in the Permian (P), which led to a porosity reduction of approximately 80.2% for O_3l [Fig. 6(h); Table 2).

Change in Error Rate

For comparison, we list the modeled porosity with and without the cementation tool and the average measured porosity data of each layer in Well ZS1 in Table 2. The error rate between the modeling and measured porosity ranged from 237.5% to 468.8% for low-porosity carbonates and from 15.0% to 19.4% for high-porosity carbonates. However, when cementation was taken into account, the error rate decreased sharply to a range of 0%–12.5% for low-porosity carbonates and 0%–5% for high-porosity carbonates (Table 2).

Discussion

Difference between Low- and High-Porosity Carbonates

The reduction percentage between the modeled porosities with and without the cementation tool for high-porosity carbonates was 16.3% and 8.7% for the Xiao'erbulake Formation (ϵ_1x) and Awatage Formation (ϵ_2a), respectively (Table 2). Neither had a reduction percentage greater than 20%. Obviously, low-porosity carbonate is significantly different from high-porosity carbonate because the porosities modeled using the cementation tool for almost every layer of low-porosity carbonate had excellent agreement with the measured data, whereas at least 70% of the modeled results without the cementation tool were underestimated significantly (Table 2). In this study, the primary porosity was less developed in low-porosity carbonates but clearly developed in high-porosity carbonates. Dolomitization played an important role in protecting or forming algal frameworks and intergranular and early hypergene dissolved pores in high-porosity carbonates (i.e., ϵ_1x and ϵ_2a), which led to a smaller reduction in porosity than in the case of the low-porosity carbonates. This mainly was because the developed dolomite skeletons triggered the protection of pore structures and prevented the porosity from decreasing while ensuring cementation (Shen et al. 2016). This difference between the low- and high-porosity carbonates should be noted to distinguish and classify the processes of model construction.

Effect on Related Parameters

Numerous studies have shown that porosity affects the petrophysical properties, including density, thickness, and thermal conductivity of strata (Sekiguchi 1984; Waples and Tirsgaard 2002), thereby influencing formation temperatures and hydrocarbon generation and preservation. The surface heat flow and thermal conductivity are related as follows:

$$q = -K\frac{dT}{dZ} \tag{1}$$

where q = surface heat flow; K = rock thermal conductivity; and dT/dZ = geothermal gradient. If q is the heat flow at any depth underground, T_0 is the surface temperature in corresponding depth Z, and the formation temperature T is as follows:

$$T = T_0 + \int_0^Z \frac{q}{K} dZ \tag{2}$$

where Z and K are functions of T (Wang 2015). According to Eq. (2), the depth and rock thermal conductivity are affected by the porosity influence the layer temperature. This supports the fact that precise porosity is an essential prerequisite for modeling, particularly for modeling huge thick Paleozoic carbonates in the Tazhong Uplift.

Therefore, based on the comparison of the results obtained by considering cementation (calibrated) and not considering cementation (uncalibrated), we found distinctions based on different parameters of burial depth, thermal conductivity, stratigraphic temperature, and vitrinite reflectance (EASY Ro%) (Fig. 7). For a comparative analysis, we examined the changes in some parameters

$$\Delta D = D_a - D_u \tag{3}$$

$$\Delta\lambda = \lambda_a - \lambda_u \tag{4}$$

$$\Delta T = \int_0^{\Delta D} \frac{q}{\Delta\lambda} dZ = Ta - Tu \tag{5}$$

$$\Delta \mathrm{VR} = \mathrm{VR}_a - \mathrm{VR}_u \tag{6}$$

where Δ represents difference; D = depth; λ = geothermal conductivity; T = strata temperature; VR = vitrinite reflectance; and subscripts a and u indicate calibrated and uncalibrated parameters, respectively. Altogether, ΔD changed from 0 to −69 m [Fig. 7(a)]; $\Delta\lambda$ changed from 0 to 0.05 W/m/K [Fig. 7(b)]; ΔT changed from −0.5 to −5.8°C [Fig. 7(c)]; and ΔVR changed from 0 to $-0.12Ro\%$ [Fig. 7(d)]. These findings illustrate that the condition of porosity dramatically affected the entire geologic model, and lower porosity always led to shallower depths, higher thermal conductivities, lower temperatures, and lower maturities.

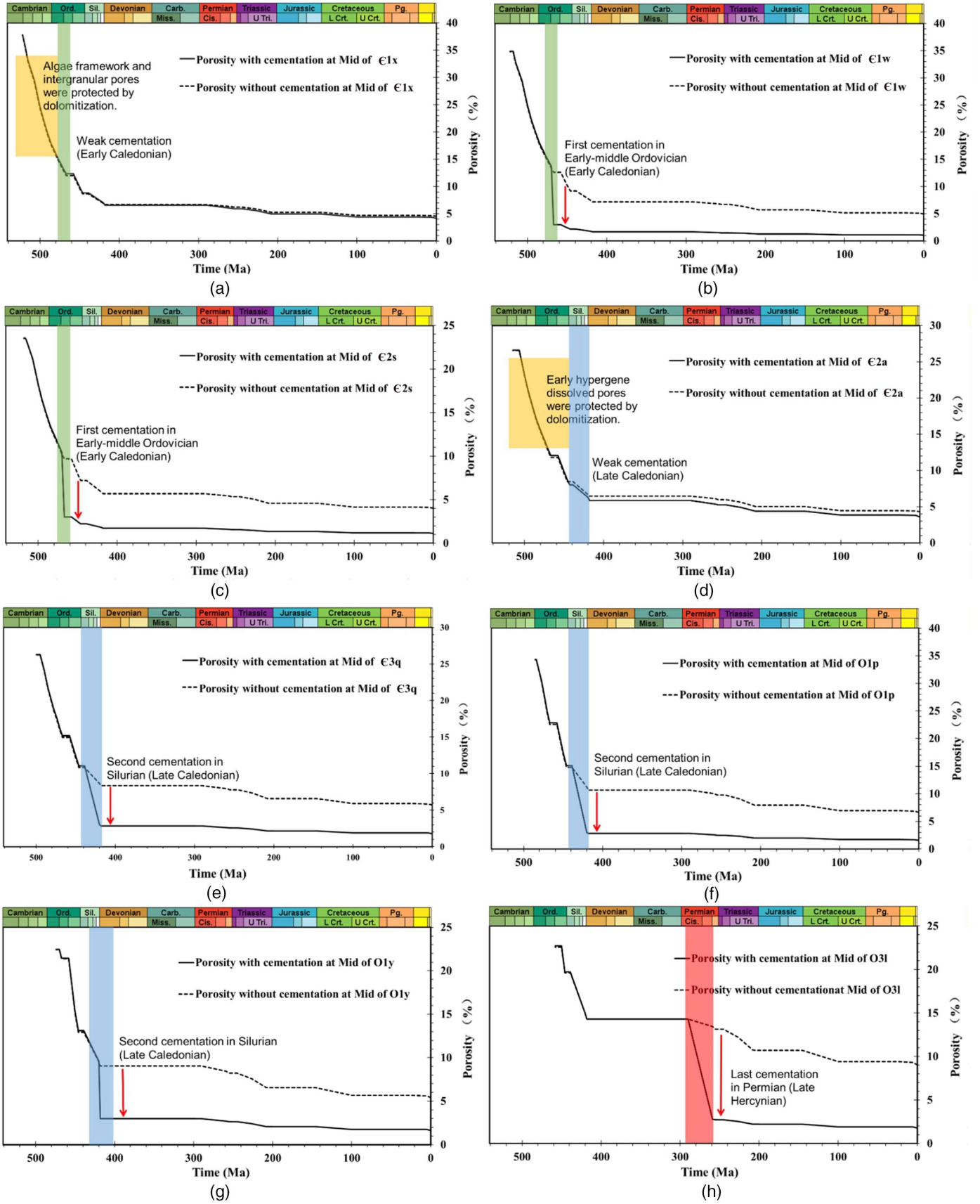

Fig. 6. Porosity evolution of different layers with and without the cementation tool.

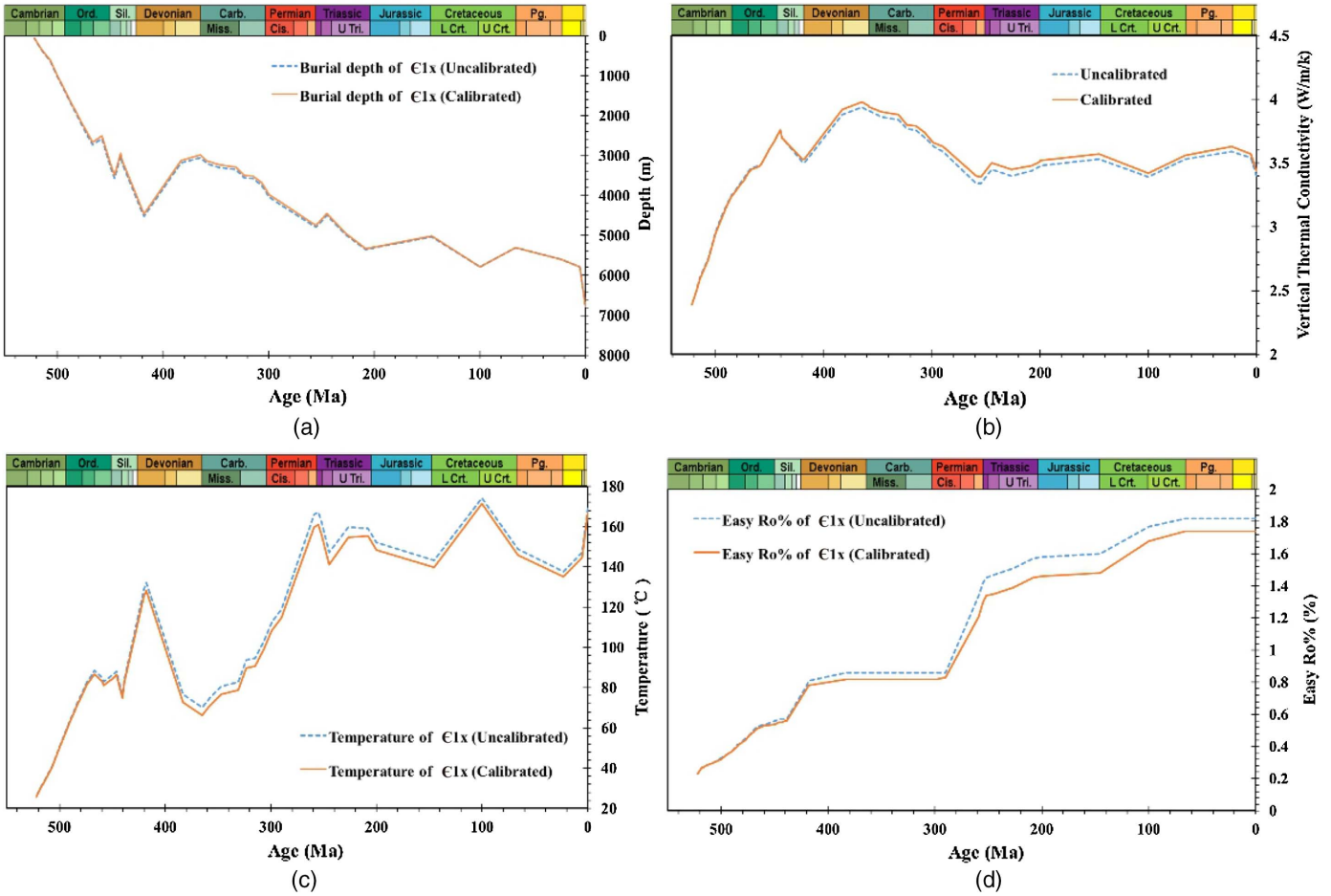

Fig. 7. Evolutionary diagrams of related parameters from the models considering and not considering cementation.

Influence on Hydrocarbon Generation

Assuming that the Xiao'erbulage Formation is the source rock, the appropriate kinetics were selected as Tang(2011)_SARA_TII (Tang et al. 1996). By setting total organic carbon (TOC) to 2% and hydrogen index (HI) to 500 mg HC/g TOC, the difference in hydrocarbon generation was calculated with (calibrated) and without (uncalibrated) the cementation tool (Fig. 8). The bulk generation mass from the cementation-considered model was always lower than that of the cementation-unconsidered model because of lower strata temperature. In this case, the early generation difference in the Caledonian was the largest (approximately 0.14 Mton); the Hercynian generation difference was in the middle range (approximately 0.03 Mton); and the last-stage generation difference was the lowest (approximately 0.01 Mton) (Fig. 8), showing that the influence of temperature change on hydrocarbon mass decreased with increasing maturity.

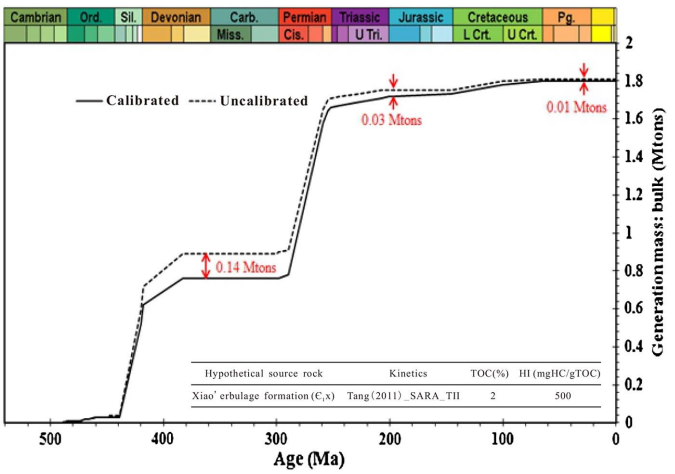

Fig. 8. Hydrocarbon generation curves from the models considering and not considering cementation.

Limitation of Cementation Tool

The aforementioned results indicate that the PetroMod version 2016.2 software outputs reasonable results of carbonate porosity modeling after considering cementation. However, in some cases, carbonate occurred not only during cementation but also during strong postdiagenesis such as in the TSR and karst processes that promoted an increase in porosity (Jiang et al. 2018; Huang et al. 2010). Hence, the cementation tool is limited for application to locations in which cementation occurs; that is, the cementation tool is applicable only to the situation of porosity reduction. However, for the process of increase in porosity in carbonates with strong postdiagenesis, other methods should be considered to model the porosity.

Conclusions

1. When performing basin modeling for thick carbonates using the PetroMod software (version 2016.2), the chemical cementation

must be taken into account, and the cementation tool is effective for dealing with the process of chemical cementation of carbonates. With the use of the cementation tool, the errors in the modeled porosity decreased significantly, demonstrating a good result for carbonate porosity modeling, which is critical for basin modeling.
2. The decrease in porosity leads to a shallower burial depth and higher thermal conductivity, ultimately resulting in a lower formation temperature and maturity. Hydrocarbon generation can be modeled more reliably after calibration, and the temperature changes affecting the hydrocarbon mass were weakened with increased maturity.
3. The carbonate porosity over time decreased rapidly because of chemical compaction. The chemical compactions occurred at different ages and to different degrees because of differences in the depositional burial time. In the case considered in this study, three major chemical cementations occurred at different ages and to various degrees in different layers; these cementations correspond to three depositional events in the Early–Middle Ordovician (Early Caledonian), Silurian (Late Caledonian), and Permian (Late Hercynian).

Data Availability Statement

Some data and models that support the findings of this study are available from the corresponding author upon reasonable request: data of measured porosity, data of lithology, kinetic model parameters, andcalibration data.

Acknowledgments

This study was supported by the Strategic Priority Research Program of the Chinese Academy of Sciences (XDA14010103), the China National Major S&T program (2017ZX05008-002-030), and the NSFC Project (41372137). The authors thank the China Scholarship Council (CSC: 201904910306) for funding them to study abroad.

References

Chen, C., Y. Wang, J. R. Beagle, L. Liao, S. Shi, and R. Deng. 2019. "Reconstruction of the evolution of deep fluids in light oil reservoirs in the Central Tarim Basin by using PVT simulation and basin modeling." *Mar. Pet. Geol.* 107 (Sep): 116–126. https://doi.org/10.1016/j.marpetgeo.2019.05.009.

Chen, D. 2008. "Structure-controlled hydrothermal dolomitization and hydrothermal dolomite reservoirs." *Oil Gas Geol.* 29 (5): 614–622. https://doi.org/10.11743/ogg20080510.

Croizé, D., F. Renard, and J. P. Gratier. 2013. "Compaction and porosity reduction in Carbonates: A review of observations, theory, and experiments." *Adv. Geophys.* 54: 181–238. https://doi.org/10.1016/B978-0-12-380940-7.00003-2.

Deng, R., C. Chen, S. Shi, and Y. Wang. 2019. "Fluid phase simulation and evolution of a condensate gas reservoir in the Tazhong Uplift, Tarim Basin." *Geofluids* 2019: 8627698. https://doi.org/10.1155/2019/8627698.

Gluyas, J., and R. Swarbrick. 2004. *Petroleum geoscience*. Hoboken, NJ: Blackwell.

Hantschel, T., and A. I. Kauerauf. 2009. *Fundamentals of basin and petroleum systems modeling*. Berlin: Springer.

Huang, H., S. Zhang, and J. Su. 2016. "Palaeozoic oil–source correlation in the Tarim Basin, NW China: A review." *Org. Geochem.* 94 (Apr): 32–46. https://doi.org/10.1016/j.orggeochem.2016.01.008.

Huang, S., Y. Gong, K. Huang, and H. Tong. 2010. "The influence of burial history on carbonate dissolution and precipitation: A case study from Feixianguan Formation of Triassic NE Sichuan and Ordovician Carbonate of Northern Tarim Basin." *Adv. Earth Sci.* 25 (4): 381–390. https://doi.org/10.11867/j.issn.1001-8166.2010.04.0381.

Huang, S., W. Sun, and P. Huang. 2009. "Chemical thermodynamics foundation of retrograde solubility for carbonate-Solution media related to CO_2." *J. Chengdu Univ. Technol.* 36 (5): 457–464. https://doi.org/10.3969/j.issn.1671-9727.2009.05.001.

Jia, C. 1997. *Tectonic characteristics and petroleum, Tarim basin, China*. Beijing: Petroleum Industry Press.

Jiang, L., R. H. Worden, and C. Yang. 2018. "Thermochemical sulphate reduction can improve carbonate petroleum reservoir quality." *Geochim. Cosmochim. Acta* 223: 127–140. https://doi.org/10.1016/j.gca.2017.11.032.

Ma, Y., T. Guo, X. Zhao, and X. Cai. 2008. "The formation mechanism of high quality dolomite reservoir in the deep of Puguang Gas Field." *Sci. China: Earth Sci.* 51 (Supply II): 53–64. https://doi.org/10.1007/s11430-008-5008-y.

Machel, H. G. 2001. "Bacterial and thermochemical sulfate reduction in diagenetic—Old and new insights." *Sediment. Geol.* 140 (1–2): 143–175. https://doi.org/10.1016/S0037-0738(00)00176-7.

Schmoker, J. W., and R. B. Halley. 1982. "Carbonate porosity versus depth: A predictable relation for South Florida." *AAPG Bull.* 66 (12): 2561–2570. https://doi.org/10.1306/03B5AC73-16D1-11D7-8645000102C1865D.

Schmoker, J. W., K. B. Krystinik, and R. B. Halley. 1985. "Selected characteristics of limestone and dolomite reservoirs in the United States." *AAPG Bull.* 69 (5): 733–741.

Schneider, F., J. L. Potdevin, S. Wolf, and I. Faille. 1996. "Mechanical and compaction model for sedimentary basin simulators." *Tectonophysics* 263 (1–4): 307–317. https://doi.org/10.1016/S0040-1951(96)00027-3.

Sekiguchi, K. 1984. "A method for determining terrestrial heat flow in oil basinal areas." *Tectonophysics* 103 (1–4): 67–79. https://doi.org/10.1016/0040-1951(84)90075-1.

Shen, A., J. Zheng, Y. Chen, X. Ni, and L. Huang. 2016. "Characteristics, origin and distribution of dolomite reservoirs in Lower-Middle Cambrian, Tarim Basin, NW China." *Pet. Explor. Dev.* 43 (3): 375–385. https://doi.org/10.1016/S1876-3804(16)30044-1.

Song, D., T. Wang, and M. Li. 2016. "Geochemistry and possible origin of the hydrocarbons from Wells Zhongshen 1 and Zhongshen 1C, Tazhong Uplift." *Sci. China Earth Sci.* 59: 840–850. https://doi.org/10.1007/s11430-015-5226-z.

Su, J., S. Zhang, H. Yang, G. Zhu, J. Mi, and Z. Xiao. 2011. "Evidence of the organic geochemistry and petrology for the adjustment process of primary reservoir: Insight into the adjustment mechanism of Hadexun oil field via Xiang-3 Well." *Acta Petrol. Sinica* 27 (6): 1886–1898.

Sun, S. 1995. "Dolomite reservoirs: Porosity evolution and reservoir characteristics." *AAPG Bull.* 79 (2): 186–204. https://doi.org/10.1306/8D2B14EE-171E-11D7-8645000102C1865D.

Tang, Y., P. D. Jenden, A. A. Nigrini, and S. C. Teerman. 1996. "Modeling early methane generation in coal." *Engergy Fuels* 10 (3): 659–671. https://doi.org/10.1021/ef950153l.

Tian, L., H. Cui, Y. Chen, J. Liu, and N. Zhang. 2015. "The distribution characteristics and prospecting significance of the Middle and Lower Cambrian dolomite reservoir in Tarim Basin." *Nat. Gas Geosci.* 26 (Supply II): 130–138. https://doi.org/10.11764/j.issn.1672-1926.2015.S1.0130.

Walderhaug, O. 2000. "Modeling quartz cementation and porosity in middle Jurassic brent group sandstones of the Kvitenbjoern field, northern North Sea." *AAPG Bull.* 84 (9): 1325–1339. https://doi.org/10.1306/A9673E96-1738-11D7-8645000102C1865D.

Wang, J. 2015. *Geothermics and its applications*. Beijing: Science Press.

Wang, Y., Y. Wen, and H. Hong. 2007. "Diagenesis of triassic feixianguan formation in sichuan basin, Southwest China." *Acta Sedimentologica Sinica* 25 (6): 831–839.

Wang, Z., H. Xie, Y. Chen, Y. Qi, and K. Zhang. 2014. "Discovery and exploration of cambrian subsalt dolomite original hydrocarbon

reservoir at Zhongshen-1 Well in tarim basin." *China Pet. Explor.* 19 (2): 1–13.
Waples, D. W., and H. Tirsgaard. 2002. "Changes in matrix thermal conductivity of clays and claystones as function of compaction." *Pet. Geosci.* 8 (4): 365–370. https://doi.org/10.1144/petgeo.8.4.365.
Xiao, Z., J. Su, H. Yang, Y. Wang, S. Huang, L. Huang, B. Zhang, N. Weng, Y. Lu, and K. Zhang. 2015. "The genesis and prospecting significance of high-sulfur gas condensates in the deep dolomite reservoirs beneath gypsum rocks: A case study of the Cambrian reservoir in Tarim Basin." *Pet. Sci. Technol.* 33 (19): 1643–1652. https://doi.org/10.1080/10916466.2015.1079537.
Yang, H. 2015. "Exploration knowledge and direction of Lower Proterozoic inner dolostones, Tarim Basin." *Nat. Gas Geosci.* 26 (7): 1213–1223.
Yang, H., Y. Chen, J. Tian, J. Du, Y. Zhu, H. Li, W. Pang, P. Yang, Y. Li, and H. An. 2020. "Great discovery and its significance of ultra-deep oil and gas exploration in well Luntan-1 of the Tarim Basin." *China Pet. Expl.* 25 (2): 62–72. https://doi.org/10.3969/j.issn.1672-7703.2020.02.007.
Ye, D., G. Wang, and Z. Lin. 2000. *Cambrian-Ordovician carbonate characteristics and prospect of oil and gas in Northern Tarim Basin*. Chengdu, China: Sichuan University Press.
Zhang, S., J. Su, X. Wang, G. Zhu, H. Yang, K. Liu, and Z. Li. 2011. "Geochemistry of Palaeozoic marine petroleum from the Tarim Basin, NW China: Part 3. Thermal cracking of liquid hydrocarbons and gas washing as the major mechanisms for deep gas condensate accumulations." *Org. Geochem.* 42 (11): 1394–1410. https://doi.org/10.1016/j.orggeochem.2011.08.013.
Zhao, W., A. Shen, J. Zheng, X. Ni, and L. Huang. 2014. "The porosity origin of dolomite reservoirs in the Tarim, Sichuan and Ordos basins and its implication to reservoir prediction." *Sci. China Earth Sci.* 44 (9): 1925–1939. https://doi.org/10.1007/s11430-014-4920-6.
Zhu, G., H. Huang, and H. Wang. 2015. "Geochemical significance of discovery in Cambrian Reservoirs at Well ZS1 of the Tarim Basin, Northwest China." *Energy Fuels* 29 (3): 1332–1344. https://doi.org/10.1021/ef502345n.
Zhu, G., J. Li, Z. Zhang, M. Wang, N. Xue, T. He, and K. Zhao. 2020. "Stability and cracking threshold depth of crude oil in 8000 m ultra-deep reservoir in the Tarim Basin." *Fuel* 282 (Dec): 118777. https://doi.org/10.1016/j.fuel.2020.118777.
Zhu, G., A. V. Milkov, J. Li, N. Xue, Y. Chen, J. Hu, T. Li, Z. Zhang, and Z. Chen. 2021. "Deepest oil in Asia: Characteristics of petroleum system in the Tarim basin, China." *J. Pet. Sci. Eng.* 199 (Apr): 108246. https://doi.org/10.1016/j.petrol.2020.108246.
Zhu, G., S. Zhang, and Y. Liang. 2005. "Isotopic evidence of TSR origin for natural gas bearing high H2S contents within the Feixianguan Formation of the northeastern Sichuan basin, southwestern China." *Sci. China Earth Sci.* 48 (11): 1960–1976. https://doi.org/10.1360/082004-147.
Zhu, G., Z. Zhang, X. Zhou, T. Li, J. Han, and C. Sun. 2019. "The complexity, secondary geochemical process, genetic mechanism and distribution prediction of deep marine oil and gas in the Tarim Basin, China." *Earth Sci. Rev.* 198 (Nov): 102930. https://doi.org/10.1016/j.earscirev.2019.102930.